MOLECULAR AND CELLULAR BIOLOGY, July 2011, p. 2742–2755 Vol. 31, No. 13
0270-7306/11/$12.00 doi:10.1128/MCB.05216-11

Distinct Properties of Human HMGN5 Reveal a Rapidly Evolving but Functionally Conserved Nucleosome Binding Protein▽

Cedric Malicet,† Mark Rochman,† Yuri Postnikov, and Michael Bustin*

Protein Section, Laboratory of Metabolism, Center for Cancer Research, National Cancer Institute, National Institutes of Health, Bethesda, Maryland 20892

Received 15 February 2011/Returned for modification 6 March 2011/Accepted 13 April 2011

The HMGN family is a family of nucleosome-binding architectural proteins that affect the structure and function of chromatin in vertebrates. We report that the HMGN5 variant, encoded by a gene located on chromosome X, is a rapidly evolving protein with an acidic C-terminal domain that differs among vertebrate species. We found that the intranuclear organization and nucleosome interactions of human HMGN5 are distinct from those of mouse HMGN5 and that the C-terminal region of the protein is the main determinant of the chromatin interaction properties. Despite their apparent differences, both mouse and human HMGN5 proteins interact with histone H1, reduce its chromatin residence time, and can induce large-scale chromatin decompaction in living cells. Analysis of HMGN5 mutants suggests that distinct domains in HMGN5 affect specific steps in the interaction of H1 with chromatin. Elevated levels of either human or mouse HMGN5 affect the transcription of numerous genes, most in a variant-specific manner. Our study identifies HMGN5 as a rapidly evolving vertebrate nuclear protein with species-specific properties. HMGN5 has a highly disordered structure, binds dynamically to nucleosome core particles, modulates the binding of H1 to chromatin, reduces the compaction of the chromatin fiber, and affects transcription.

Dynamic changes in chromatin structure play a key role in epigenetic regulation and in the orderly progression of transcription, replication, recombination, and repair. Chromatin dynamics are facilitated by the combined action of numerous nuclear components. These include nuclear proteins that reversibly modify specific histone residues, ATP-dependent nucleosome remodeling complexes, and structural proteins that modify the architecture of their chromatin binding sites. Structural chromatin architectural proteins, such as the linker histone H1 (7, 42) and members of the high-mobility-group (HMG) protein superfamily (3, 6), are known to bind dynamically to nucleosomes and to affect the structure and function of chromatin. Significantly, the chromatin binding of histone H1 variants and of all the members of the HMG protein superfamily is interdependent: these proteins function within a dynamic network where the binding of one protein affects the binding of other members of the network (10, 11). Therefore, it is important to characterize the chromatin interaction of each member of this network of nucleosome-binding proteins. Here we describe the unique properties and chromatin interactions of human HMGN5 (hHMGN5).

The HMG superfamily, whose members are among the most abundant and ubiquitous vertebrate nonhistone chromosomal proteins, is subdivided into three families: HMGA, HMGB, and HMGN (3, 6). The HMGN family is made up of nuclear proteins that bind without any DNA sequence specificity (5) to the 147-bp nucleosome core particle (CP), the building block of the chromatin fiber. HMGNs bind to nucleosomes through a conserved protein domain, the nucleosome binding domain (NBD). Embedded in this domain is a highly conserved decapeptide sequence which is absolutely necessary for the specific interaction of HMGNs with the CP (39). The binding of HMGNs to nucleosomes affects chromatin-related processes such as transcription, replication, and repair (2, 4, 5, 16, 20, 27, 41, 43). HMGNs may mediate these effects by causing a change in chromatin structure (5, 27) or the level of histone posttranslational modifications (22, 23), by affecting ATP-dependent chromatin remodeling activities (30), or by a combination of these.

The HMGN protein family consists of 5 members, HMGN1 to -5, which have been detected only in vertebrates. The genes coding for these proteins have similar structures, suggesting that they evolved from a common ancestor. The HMGN1, HMGN2, HMGN3, and HMGN4 proteins contain fewer than 100 amino acids, and each has a distinct sequence that is highly conserved throughout the animal kingdom (5, 27). HMGN5, which is the most recently discovered HMGN variant (32, 34), differs from the other HMGN members in both size and sequence conservation. For example, mouse HMGN5 (mHMGN5) contains 406 amino acids, including a highly acidic, 300-amino-acid C terminus, and is 4 times larger than the other HMGN variants (35). Furthermore, although the NBD of mHMGN5 is similar to that of the other HMGN variants, its cellular location is distinct in that it is excluded from heterochromatin, unlike the other HMGNs (31). Analysis of the gene coding for hHMGN5 suggests that the protein differs from the mouse homologue (21), raising the possibility that the chromatin binding and function of hHMGN5 are also distinct from those of the mouse homologue; however, so far, only the mHMGN5 protein has been purified and studied in detail.

Here we report that HMGN5 is a rapidly evolving variant of the HMGN nucleosome-binding protein family with a C-ter-

* Corresponding author. Mailing address: Protein Section, Laboratory of Metabolism, Center for Cancer Research, National Cancer Institute, National Institutes of Health, Bethesda, MD 20892. Phone: (301) 496-5234. Fax: (301) 496-8419. E-mail: bustin@helix.nih.gov.
† C.M. and M.R. contributed equally to this study.
▽ Published ahead of print on 25 April 2011.

minal sequence that is highly divergent among various vertebrate species. We characterized hHMGN5 and demonstrated that in contrast to mHMGN5, which localizes to euchromatin, hHMGN5 localizes to both eu- and heterochromatin, similar to other HMGN proteins. Analysis of deletion and swap mutants indicated that the C-terminal regions of the proteins determine their specific chromatin locations and nucleosome interactions. Furthermore, we demonstrated that the negatively charged C terminus of hHMGN5 interacts with the positively charged C terminus of H1 and that the hHMGN5 protein reduces the compaction of chromatin in a fashion analogous to that for the mouse variant. Both human and mouse HMGN5 proteins reduce chromatin compaction and affect the cellular transcription profile; however, mHMGN5, which localizes to euchromatin (32), affects the transcription of many more genes than hHMGN5 localized to heterochromatin. Thus, although both the human and mouse proteins counteract the chromatin-condensing activity of histone H1, their effects on the cellular phenotype may be species specific.

MATERIALS AND METHODS

Cell culture, transfection, and siRNA treatment. Simian virus 40 (SV40)-transformed mouse embryonic fibroblasts (MEFs), 293T cells, and MDAMB231 cells were purchased from the ATCC and were used for either microscopy, fluorescence recovery after photobleaching (FRAP) experiments, or microarrays. For the Lac operon experiment, the stable cell line NIH2/4 was a gift from the lab of Tom Misteli, NCI. NIH2/4 cells carry an array of 256 copies of the Lac repressor binding sequence and 96 copies of the tetracycline response element sequence. Cells were maintained in Dulbecco's modified Eagle's medium (DMEM; Invitrogen, Carlsbad, CA) with 10% fetal calf serum (FCS; Invitrogen). Stable MDAMB231 cell lines were prepared using a retrovirus generated by transient transfection of amphotropic helper Phoenix cells with a retrovirus containing the wild-type human or mouse HMGN5 protein. The retroviral supernatant was then collected and added to MDAMB231 cells with 0.8 μg/ml Polybrene (Chemicon International). An empty vector was used as a control. Selection of stable clones was done using 1 μg/μl puromycin (Sigma) for 2 weeks. For small interfering RNA (siRNA)-mediated downregulation of HMGN5, 293T cells were transfected with a specific siRNA (L-014649-01-0005) or control siRNA (D-001810-10-05) On Target Plus Smart pool from Dharmacon, using Dharmafect 4 transfection reagent (Dharmacon, Thermo Scientific). Following initial transfection, cells were grown for 48 h. Cells were collected 24 h and 48 h after transfection of siRNA.

Antibodies. Anti-hHMGN5 antibody (produced in rabbits and affinity isolated; Prestige Antibodies) was supplied by Sigma Life Science (HPA000511). Anti-actin (clone) AC-74 was obtained from Sigma (A5316). Secondary antibodies for microscopy were purchased from Jackson Immunoresearch. Horseradish peroxidase (HRP)-conjugated secondary antibodies for Western blots were purchased from Millipore.

Plasmids and construction. Sequences used for this study were for human HMGN5 (GenBank accession no. NM_030763.2) and mouse HMGN5 (GenBank accession no. NM_016710). The sequence referred to as hHMGN5 (S19,23E) is an NBD mutant with the two serines at positions 19 and 23 mutated to two glutamic acid residues (KRR*S*ARL*S*AMLV to KRR*E*ARL*E*AMLV). hHMGN5-YFP, hHMGN5(S19,23E)-YFP, and mHMGN5-YFP fusion proteins were cloned into a pEYFP-N1 vector (Clontech). Briefly, the HMGN5 insert was amplified with two primers containing BamHI at the 5′ end and Xho at the 3′ end and then ligated to the vector, which was cut by BglII at the 5′ end and by Xho at the 3′ end. LacR-CFP and H1-GFP plasmids were gifts from the laboratory of T. Misteli (NIH, NCI). Construction for the Lac operon experiment was done as follows: mHMGN5 and hHMGN5 were cloned in frame with the N terminus of the LacR-CFP construct by using NheI and AgeI restriction enzymes. A retrovirus pMCS vector (Cell Biolabs, Inc.) was used to produce the stable MDAMB231 cell line.

Confocal microscopy and FRAP analysis. Cells were plated on poly-D-lysine-coated coverslips on 6-well plates for imaging of fixed cells. For FRAP experiments and localization in living cells, cells were plated on MatTek glass-bottomed culture dishes 24 h before transfection. During the experiment, cells were kept at 37°C. Twenty-four hours after transfection, the binding affinities of all HMGN5 variants, including human, mouse, and several mutant variants, were analyzed by FRAP. Confocal images were collected using a Zeiss LSM 510 system mounted on a Zeiss Axiovert 200 M microscope (Carl Zeiss Inc., Thornwood, NY) using an oil-immersion Plan-Apochromat ×63/1.4 differential interference contrast (DIC) objective lens. Colocalization of proteins with DNA was analyzed using the LSM Image analysis program. FRAP analysis was performed with a Zeiss LSM 510 confocal microscope using the 488-nm line of an argon laser and the 543-nm line of a HeNe laser as described previously (25). Typically, 2 prebleach images were acquired, followed by a double-bleach pulse of 10 iterations, using a spot of 30 μm in diameter. Single images were then collected. For imaging, the laser power was set to 0.1% of a 25-mW argon laser (488-nm line), and for bleaching, the laser power was set to 100%. FRAP recovery curves were generated from background-subtracted images. The total fluorescence was determined for each image and compared to the initial total fluorescence to determine the amount of fluorescence lost during bleaching and imaging. The fluorescence intensity in the bleach area was normalized to the initial fluorescence in the bleach area. In a typical experiment, several spots in 6 to 10 cells were used for FRAP. Each experiment was repeated at least three times. Competitive FRAP experiments were performed with BALB/c 3T3 cell lines stably expressing H1.0-GFP (25).

Western blots. Whole-cell lysates were prepared in 1× SDS-PAGE sample buffer (Bio-Rad) supplemented with protease inhibitors. The samples were fractionated in 10% precast Criterion gels, transferred by a semidry method to a polyvinylidene difluoride (PVDF) membrane, blocked with nonfat milk (5%) in 1× phosphate-buffered saline (PBS), and probed with antibodies. Chemiluminescence detection using Immobilon Western was performed according to Millipore recommendations.

Salt extraction. SV40-transformed MEFs transfected with either hHMGN5-YFP or mHMGN5-YFP were first washed in 1× PBS and then washed 3 times in washing buffer (20 mM HEPES, pH 7.0, 10 mM KCl, 10 mM $MgCl_2$, 20% glycerol, 0.1% Triton X-100, 0.5 mM dithiothreitol [DTT], 1 mM orthovanadate, Complete protease inhibitor, 0.25 mM phenylmethylsulfonyl fluoride [PMSF]). Finally, cells were resuspended in 200 μl of the washing buffer, and NaCl was added to final concentrations of 0 mM, 125 mM, and 250 mM. Extraction was performed on ice for 15 min, with mixing every 2 to 3 min. Cells were centrifuged at 15,000 × *g* for 5 min. The pellet and the supernatant fraction were collected in 1× SDS-PAGE sample buffer (Bio-Rad) supplemented with protease inhibitors, followed by brief sonication and boiling.

Microarray expression analysis. MDAMB231 stable clones overexpressing HMGN5 or control empty retroviral vector were used for microarray expression analysis. RNA was prepared as described previously (32). Expression analysis was performed using an Affymetrix U133 Plus GeneChips 430 2.0 human array at the Laboratory of Molecular Technology (LMT), NCI, Frederick, MD. Microarray expression data were analyzed by BRB Array Tools GeneSpringGX software. A P value of <0.001 was set as a threshold for significant transcriptional changes. Network analyses were performed using MetaCore network building tools (GeneGo Inc., St. Joseph, MI).

Chemical cross-linking. *HMGN5* was cloned into pGEX4T2 at BamHI and EcoRI sites, and *Hmgn5* was cloned as previously described (32). All proteins were expressed in bacteria as previously described (34). Histone H5 was purified from chicken erythrocytes by acid extraction and Mono S ion-exchange chromatography. Chemical cross-linking between purified HMGN5 and histone H5 was performed as described previously (14). Briefly, the purified proteins were mixed at a final concentration of 2 μM in 150 mM NaCl, triethanolamine-HCl buffer, pH 8.0, cross-linked by 100 μM dimethyl suberimidate dihydrochloride (DMS; Sigma-Aldrich) for 60 min at room temperature, and fractionated in precast 15% SDS-PAGE Criterion gels (Bio-Rad Laboratories). Gels were then stained with Coomassie blue (Biosafe Coomassie; Bio-Rad).

Gel retardation analysis. Nucleosome core particles were purified from chicken red blood cell nuclei as described previously (32). Recombinant HMGN protein (20 to 200 nM) was incubated with 50 nM core particles in 5 μl 2× Tris-borate-EDTA (TBE) with 2% Ficoll for 15 min on ice. Samples were then loaded directly onto a 5% polyacrylamide gel made in 2× TBE and electrophoresed at 4°C. A parallel lane containing bromphenol blue and xylene cyanol dyes was run to measure the migration distance. After electrophoresis, gels were stained with SYBR gold stain (Molecular Probes) and photographed using a yellow photographic filter (28).

RESULTS

HMGN5 is a rapidly evolving protein. A query of PubMed databases detected HMGN5 transcripts in only five species:

Homo sapiens (hHMGN5), *Mus musculus* (mHMGN5), *Rattus norvegicus*, *Pan troglodytes*, and *Bos taurus*. In all species, the gene coding for HMGN5 is located on chromosome X, in a locus that also contains the *BRWD3* and *SH3BGRL* genes (Fig. 1A). The syntenic location of *HMGN5* on chromosome X in all species examined provides additional evidence that the *HMGN5* genes are orthologous. A query of the *Gallus gallus* genome with the highly conserved NBD of the HMGN protein family confirmed the absence of an *HMGN5* gene. Thus, the *HMGN5* gene evolved after the divergence of the mammalian and avian branches approximately 300 million years ago (40).

Comparative sequence analysis and searches of the PROSITE database (18) revealed that the structures of the HMGN5 gene and protein are highly similar to those of the other known HMGN genes and proteins (27). All HMGN5 proteins contain a nuclear localization signal (NLS) encoded by exon I, a positively charged NBD encoded by exons III and IV, and a long acidic tail in the C-terminal region, most of which is encoded by exon VI. Embedded in the NBD is a highly conserved 10-amino-acid sequence (RRSARLSA[RK]P) which is encoded by exon III, and we defined this as the NBD core (c-NBD) (Fig. 1B). The c-NBD, which serves as the signature of the HMGN protein family (9), anchors the binding of HMGN proteins to nucleosome core particles (39).

Although the HMGN5 proteins are clearly related, their amino acid sequence is surprisingly variable. While the NLS encoded by exon I and the NBD core encoded by exon III are highly conserved, the sequence encoded by exon II is highly variable. Likewise, the regions encoded by exons IV, V, and VI are significantly more variable in HMGN5 proteins than in other members of the HMGN protein family. One of the most prominent characteristics of HMGN5 is the high content of charged amino acids and their asymmetric distribution throughout the primary sequence. While the N-terminal 50 amino acids contain 3 times more positively charged than negatively charged amino acids, the C-terminal regions, which are highly variable in length, all have a highly negative net charge (Fig. 1B). Exon VI, which in all HMGN5 genes encodes more than 50% of the protein, contains the repetitive motif EDGKE; the mouse C-terminal region contains 11 repeats, while the *Bos taurus* and *Pan troglodytes* versions contain only 3 repeats. Over 70% of this tail is composed of the four amino acids DEGK. In spite of these similarities, the sequence and size of this region differ greatly among the HMGN5 proteins (Fig. 1B). The sequence variability may be related to the presence of retrotransposon sequences in exon VI. It has been suggested that HMGN5 originated from an insertion of an ancestral HMGN gene into a locus with a low recombination frequency in chromosome X and the subsequent insertion of retrotransposons into this genomic region (21). The X chromosome is known to be a preferential site for retrotransposition of both human and mouse genes (19).

The high sequence variability among the HMGN5 proteins raises the question of the degree of functional similarity between the proteins. Here we focus on the human HMGN5 variant and compare it to the mouse HMGN5 variant, whose function was characterized previously (32). Schematic alignment of the genes coding for the mouse and human proteins revealed that the most prominent difference between the proteins is in their C-terminal regions, which are encoded by exon VI (Fig. 1C). In particular, the C terminus of mHMGN5 is significantly longer and more acidic and contains 3 times as many EDGKE repeats as the human protein. The 3′-untranslated region (3′UTR) of hHMGN5 represents approximately 44% of the entire cDNA (951 of 2,126 bp), is longer than the 3′UTR of mHMGN5, and contains 3 different polyadenylation sites (21). In summary, the properties of the C-terminal region not only distinguish the HMGN5 variant from all other HMGN variants but also lead to species-specific differences in the properties of the HMGN5 variant.

Distinct intranuclear organization of human and mouse HMGN5 proteins. hHMGN5 was detected in a Western blot as a single band of 55 kDa, which is considerably higher than 31 kDa, the calculated molecular mass of hHMGN5 (Fig. 2A, left panel). We also noted that the electrophoretic mobility of mHMGN5 was anomalously high, since the 406-amino-acid protein, with a calculated molecular mass of 44.6 kDa, was visualized as a 75-kDa band (Fig. 2A) (32). To ensure the specificity of the antibody, we treated the cells with siRNA specific for hHMGN5. The siRNA led to marked reduction of the 55-kDa band, thereby confirming the specificity of the antibody (Fig. 2A, right panel).

A distinctive feature of the mHMGN5 protein is its preferential localization to euchromatin (32); all other members of the HMGN family are distributed throughout the nucleus but preferentially localize to heterochromatin. Immunostaining of endogenous hHMGN5 in human 293T cells revealed a prominent colocalization with Hoechst staining (Fig. 2B, panels a to f) and a slightly diffuse localization throughout the rest of the nucleus, a pattern similar to that previously observed for all members of the HMGN family except for mHMGN5. A similar pattern was observed by confocal microscopy in human U2OS cells cotransfected with vectors for HMGN5-YFP and HP1β-cherry, a protein known to be enriched in constitutive heterochromatin. The hHMGN5 protein colocalized with HP1β, while mHMGN5 did not (Fig. 2C, panels a to f). The differences between human and mouse HMGN5 proteins were even more obvious when the cells were stained with propidium iodine (PI). In cells overexpressing hHMGN5, PI stained discrete heterochromatic regions which colocalized with YFP-hHMGN5 (Fig. 2D, panels a to c). In contrast, in cells expressing mHMGN5, the discrete heterochromatic regions were lost and the PI stain did not produce discrete peaks (Fig. 2D, panels d to f), suggesting that mHMGN5 altered the higher-order chromatin organization. Confocal microscopy of MEFs confirmed that the nuclear organization of hHMGN5 is distinct from that of mHMGN5 (Fig. 2E, panels a to f). The localization profiles demonstrate that while hHMGN5-YFP colocalizes with the highly condensed constitutive heterochromatin DNA, mHMGN5-YFP does not, a finding that supports previous observations (32). In summary, the intranuclear organization of hHMGN5 is different from that of mHMGN5; the former localizes preferentially to heterochromatin, while the latter leads to a loss of heterochromatin and is located preferentially in euchromatin.

Distinct nucleosomal interactions of human and mouse HMGN5 proteins. HMGNs are known to specifically recognize the generic structure of the 147-bp CP, the building block of the chromatin fiber. Mobility shift assays (15) revealed that at a physiological salt concentration (150 mM NaCl), the HMGN

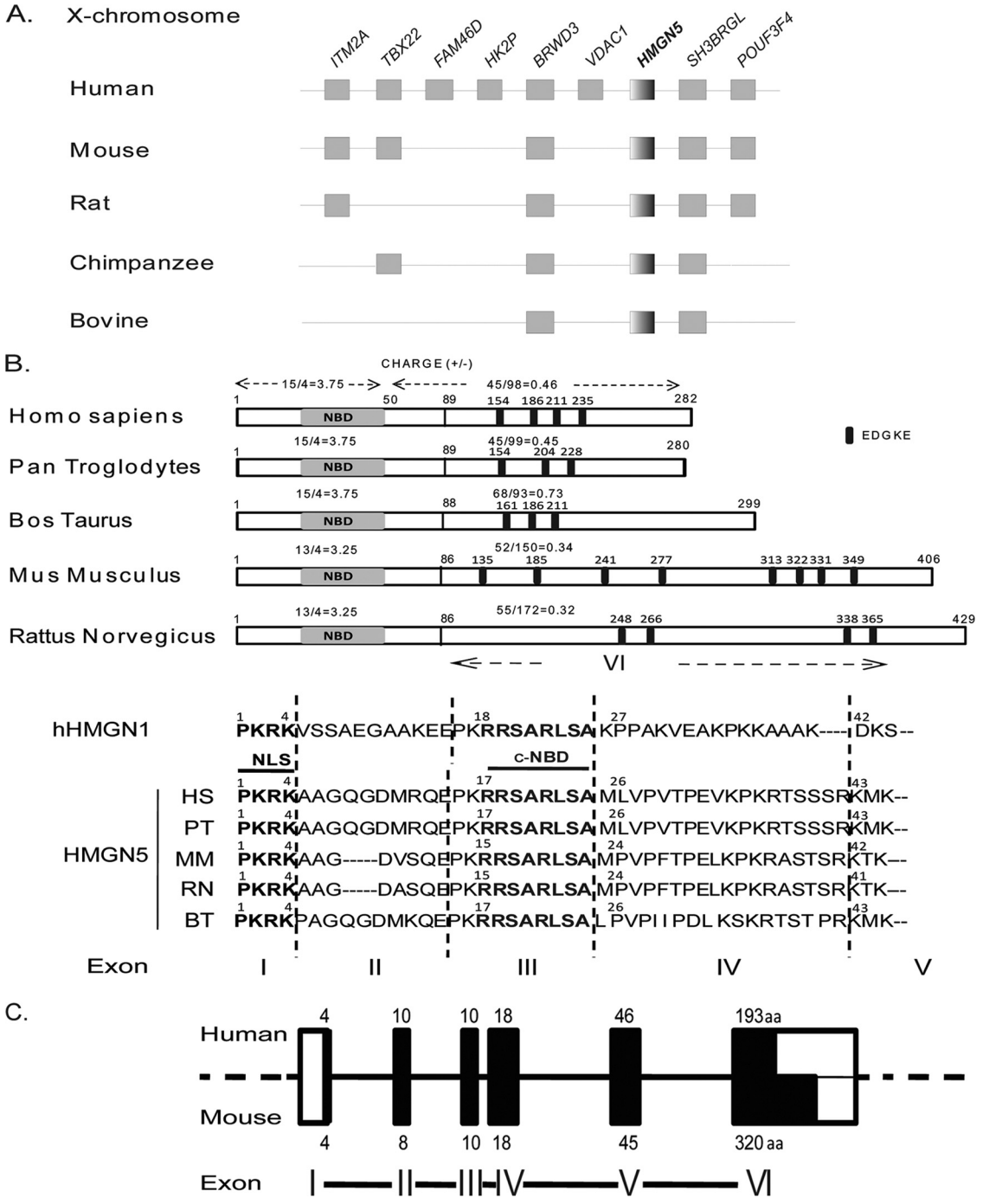

FIG. 1. Sequence comparison and analysis of orthologous HMGN5 proteins and genes. (A) Syntenic location of HMGN5 genes on chromosome X in various species. (B) Outline of HMGN5 protein structure in various species. The position of the conserved nucleosome binding domain (NBD) is indicated. The position of the first amino acid of exon VI is indicated above the sequence. Black boxes indicate the approximate positions of the repetitive sequence motif EDGKE, and the numbers above the boxes indicate the position of the first E in each motif. In *Pan troglodytes*, several HMGN5 isoforms have been detected; for the alignment presented in panel B, we selected the isoform that has 91% amino acid identity with the human protein. The numbers of positively and negatively charged amino acids and the net charges in the first 50 N-terminal amino acids and in the rest of the protein are indicated above each sequence outline. The sequence below the outline depicts the first 4 exons. The conserved NLS at the N terminus and the invariable c-NBD are indicated. Vertical lines demarcate the exon-intron boundaries. (C) Outlines of human and mouse HMGN5 genes (31). Black boxes represent the exons, and white boxes represent the 5′ and 3′ untranslated regions. The number of amino acids encoded by each exon is indicated.

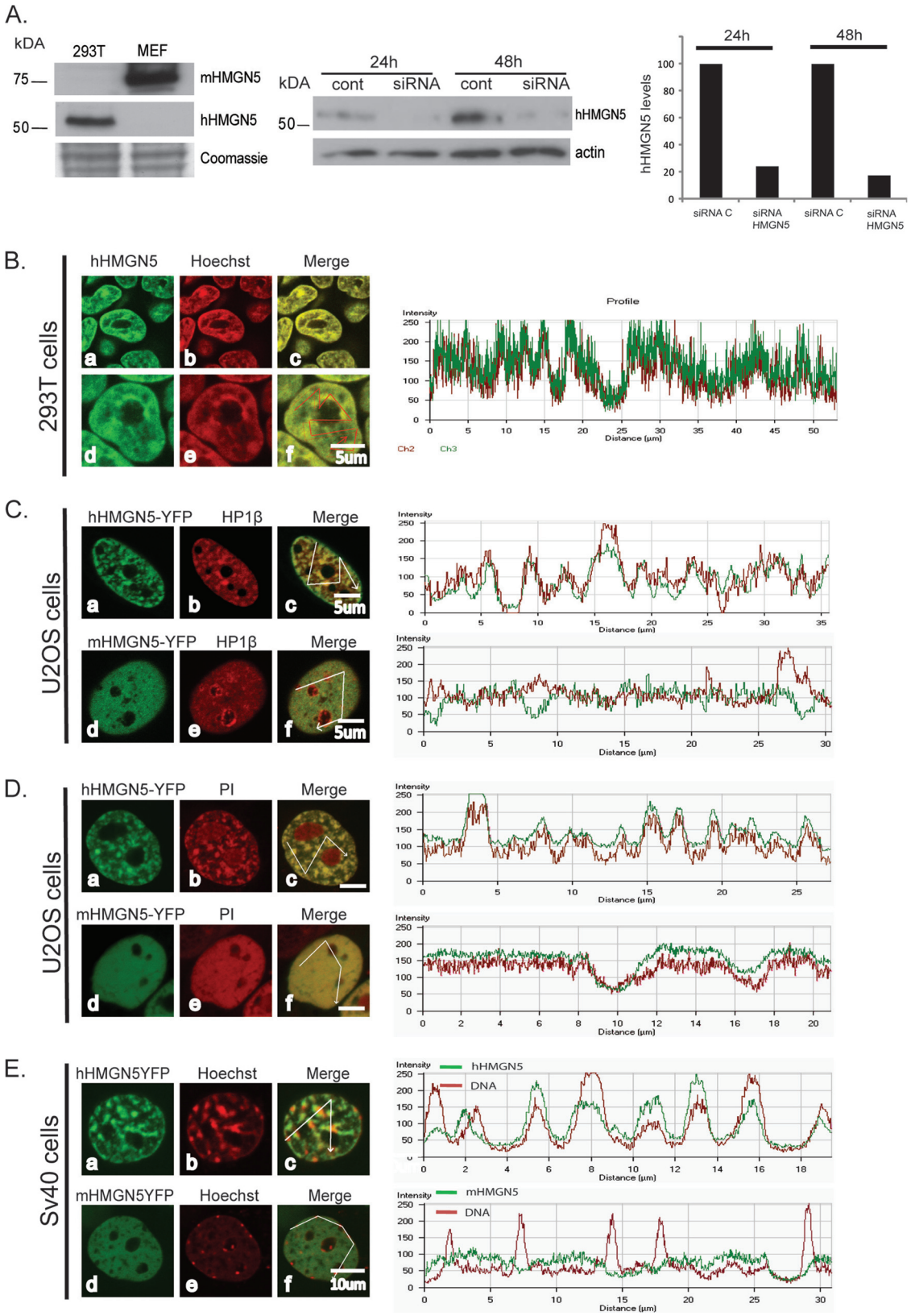

FIG. 2. Distinct nuclear locations of human and mouse HMGN5 proteins. (A) The left panel depicts a Western blot analysis of the endogenous mouse protein (in MEFs) and human protein (in 293T cells). Coomassie blue staining indicates equal protein loading. The center panel depicts Western blots of extracts from 293T cells after treatment with siRNA against human HMGN5 for the indicated times. Loss of the protein confirms the specificity of the antibody. The bar graph on the right presents quantification of the protein level normalized to actin. The protein levels in

variants bound specifically to CPs and formed complexes that contained only one type of HMGN protein. Accordingly, the addition of an equimolar mixture of HMGN1 and HMGN2 to CPs resulted in complexes that contained one CP and two molecules of either HMGN1 or HMGN2. CP complexes that contained one molecule of HMGN1 and one of HMGN2 were not detected (29). Likewise, the addition of HMGN2 and mHMGN5 to purified CPs resulted in complexes that contained either two molecules of HMGN2 or two molecules of mHMGN5 (34). These studies suggested that each HMGN variant has unique properties and forms specific complexes with CPs.

To examine whether mouse and human HMGN5 proteins have distinct properties and form distinct complexes, we first tested whether hHMGN5 alone forms complexes with purified CPs. Mobility shift assays revealed that like all other HMGNs, hHMGN5 at physiological ionic strengths bound cooperatively to CPs and formed complexes that contained two molecules of hHMGN5 per CP (Fig. 3A, left panel). To test whether hHMGN5 and mHMGN5 form specific or mixed complexes, we added CPs to an equimolar mixture of the two proteins. As shown in Fig. 3A (right panel), two distinct complexes were formed. One complex had the mobility of CP plus 2 molecules of hHMGN5, while the other migrated as CP plus 2 molecules of mHMGN5; heterodimeric complexes of CPs with one hHMGN5 and one mHMGN5, which would have an intermediate mobility, were not observed. Thus, the interaction of protein with CPs is specific to each HMGN5 variant.

To gain insights into the interactions of human and mouse HMGN5 proteins with chromatin in living cells, we expressed yellow fluorescent protein (YFP)-labeled proteins in SV40-transformed MEFs and used confocal fluorescence microscopy to visualize their locations. This analysis revealed that while wild-type hHMGN5-YFP clearly localized to heterochromatin, the double point mutant hHMGN5(S19,23E), which cannot bind to nucleosomes because of mutation of the two serines in the NBD (39), was evenly distributed throughout the nucleus, similar to mouse HMGN5 (Fig. 3B). This observation indicates that the specific interaction with nucleosomes defines the localization pattern of hHMGN.

Next, we used FRAP to measure the relative mobilities of the proteins in the cells. The rate of FRAP is known to be inversely proportional to the time an HMGN molecule resides on chromatin, and HMGN mutants that do bind to nucleosomes have a very short residency time (10, 31). FRAP analysis revealed that the residency time of hHMGN5 in heterochromatin was significantly longer than that in euchromatin. In contrast, hHMGN5(S19,23E), which does not bind to chromatin, had an extremely short residence time, an indication that the protein interacts with chromatin through its c-NBD (Fig. 3C). The time necessary to recover 70% of the initial fluorescence (t_{70}) of hHMGN5 in heterochromatin was 15 s, while that in euchromatin was only 3.6 s, a 4-fold difference (Fig. 3C). Mouse HMGN5 does not bind to heterochromatin, localizes mostly to euchromatin (31), and has a t_{70} of 1.6 s, significantly shorter than that of hHMGN5 (Fig. 3C). We also noted that while the fluorescence of mHMGN5 recovered fully, that of hHMGN5 did not recover fully in either hetero- or euchromatin, an indication of a very slow, highly immobile fraction that binds to chromatin with a long residence time. Indeed, salt extraction analysis revealed that the mHMGN5 protein bound more weakly to chromatin than the human protein did. A significant portion of the mouse protein leaked out of the nucleus at very low NaCl concentrations, and already at 125 mM NaCl, only around 20% of the mHMGN5 protein remained chromatin bound (Fig. 3D). In contrast, around 40% of the hHMGN5 protein remained bound to chromatin even at 250 mM NaCl.

Taken together, the results indicate that although both human and mouse HMGN5 proteins bind specifically to the 147-bp nucleosome CP, their chromatin interactions are distinct. The proteins form distinct complexes with CPs, mHMGN5 has a higher FRAP recovery rate, and mHMGN5 is extracted from chromatin at lower NaCl concentrations than those with hHMGN5.

The C-terminal domain distinguishes hHMGN5 from mHMGN5. The largest difference between the human and mouse HMGN5 proteins is found in the C-terminal domain, most of which is encoded by exon VI. ClustalW alignment revealed that while the regions encoded by the first 5 exons (89 amino acids in hHMGN5 and 86 amino acids in mHMGN5) have sequences with 67% identity, the shared identity is less than 47% in the rest of the protein. The C-terminal domain of mHMGN5 is 319 amino acids long and contains 11 EDGKE repeats, while that of hHMGN5 has 192 amino acids and contains only 4 EDGKE repeats. Furthermore, the C-terminal domain of mHMGN5 is more negatively charged, with a base-to-acid charge ratio of 0.32, compared to 0.46 for hHMGN5. To test whether the C terminus is the underlying reason for the differences in nuclear organization and chromatin binding, we produced truncated versions of both the mouse and human HMGN5 proteins containing only the first 66 amino acids. These truncated mutants, named hHMGN5ΔC and mHMGN5ΔC, which contained the entire NBD of the proteins, had 67% (44/66 amino acids) sequence identity and 79% similarity.

Confocal fluorescence microscopy of cells that expressed the truncated proteins revealed that both proteins localized mostly

cells treated with control siRNA were set to 100%. (B) Nuclear localization of human HMGN5. (a to f) Endogenous HMGN5 protein visualized by immunofluorescence (green) and DNA visualized by Hoechst staining. The merged images and their localization profiles indicate that HMGN5 colocalizes with heterochromatin. (C and D) Dissimilar localization and chromatin effects of hHMGN5 and mHMGN5 in human U2OS cells transfected with YFP-labeled HMGN5. Heterochromatin was visualized by HP1β-cherry (C), and DNA was visualized by propidium iodide staining (D). The scans show colocalization profiles along the paths depicted by the lines drawn in the panels showing the merged fluorescence images. Note the lack of discrete heterochromatic regions in cells transfected with mHMGN5. (E) Dissimilar nuclear localization of mouse and human HMGN5 proteins in mouse embryonic fibroblasts transfected with YFP-labeled HMGN5 and counterstained with Hoechst stain. Merged images and localization profiles confirm that human HMGN5 localizes preferentially to heterochromatin, while mouse HMGN5 is depleted from the densely stained heterochromatic dots.

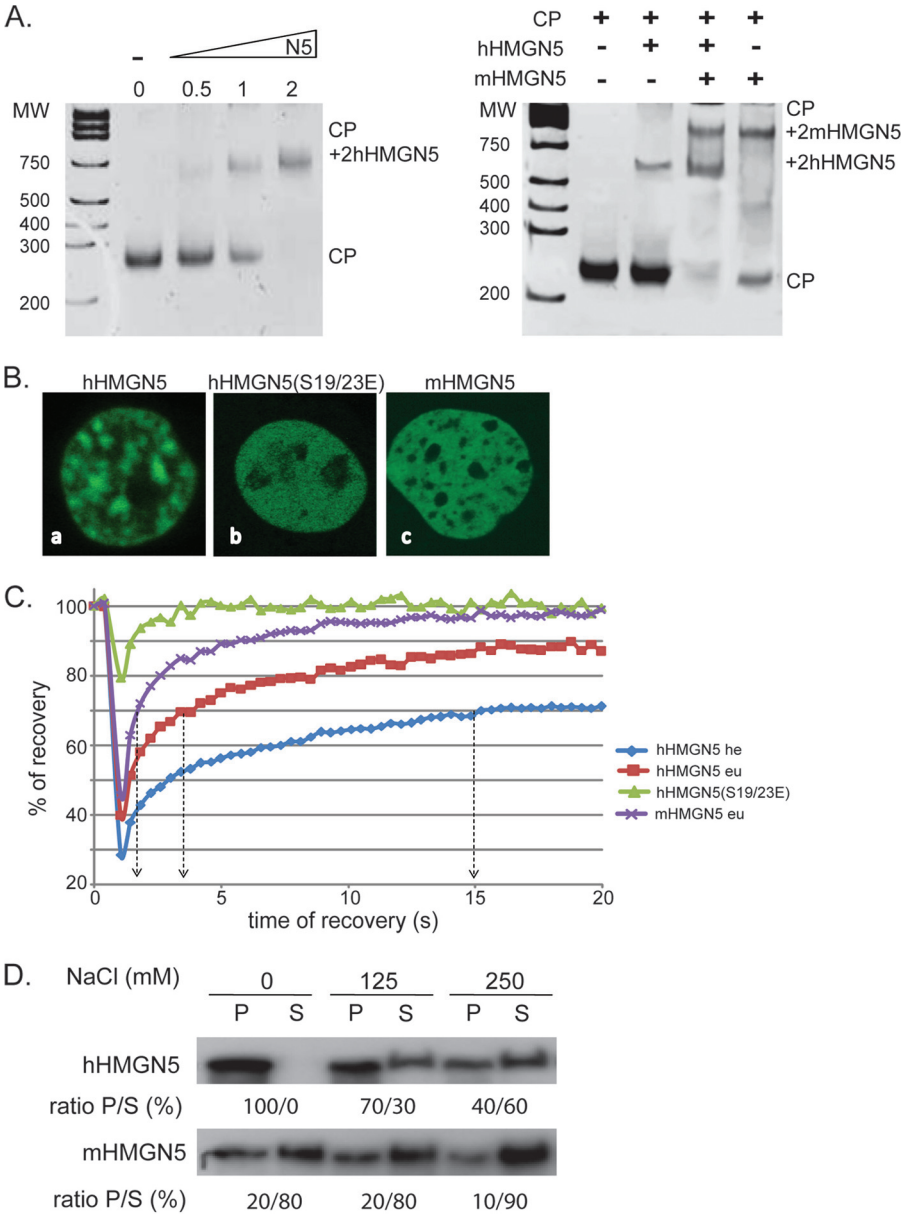

FIG. 3. Binding of HMGN5 to nucleosome CPs. (A) (Left) Mobility shift assay of CP with increasing concentrations of recombinant human HMGN5 under cooperative conditions at the molar ratio indicated above each lane. (Right) Mobility shift assay of nucleosome core particles with mixed human and mouse HMGN5 proteins. Only homodimeric CP plus 2 hHMGN5 or CP plus 2 mHMGN5 was detected. (B) Fluorescence images depicting the intranuclear distribution of hHMGN-YFP (a); hHMGN5(S19,23E)-YFP, which does not bind to chromatin (b); and mHMGN5-YFP (c). (C) FRAP recovery curves for hHMGN5-YFP, hHMGN5(S19,23E)-YFP, and mHMGN5-YFP in either euchromatin (eu) or heterochromatin (he). In living cells, hHMGN5-YFP and mHMGN5-YFP bind to chromatin with different affinities. The extremely fast recovery of the FRAP signal for the hHMGN5(S19,23E) mutant indicates that this mutant does not bind to chromatin. The t_{70} values for various HMGN5 variants are indicated by broken lines. (D) Salt extraction of HMGN5 recombinant proteins. Proteins were salt extracted from cells with increasing NaCl concentrations. Supernatants (S) and pellets (P) were collected for each sample and probed by Western blotting with antibodies to either hHMGN5 or mHMGN5.

to heterochromatin (Fig. 4A), just like all other members of the HMGN family except for mHMGN5. The localization profiles clearly indicated a correlation between the relative intensities of the signals obtained from the truncated proteins and DNA. Thus, the different chromatin localization of hHMGN5 and mHMGN5 is due to their different C-terminal regions.

FRAP analysis of the truncation mutants further demonstrated the significance of the C-terminal region of the protein in determining the unique properties of mouse and human HMGN5 proteins. While the fluorescence recovery profiles of the wild-type proteins differed greatly, those of their C-terminal deletion mutants were very similar. Thus, the t_{60} (time necessary to recover 60% of original fluorescence) of mHMGN5 was 2 s, while that of hHMGN5 was more than 15 s. In contrast, the t_{60} of hHMGN5ΔC was 4 s, while that of mHMGN5ΔC was 3.5 s (Fig. 4B). Thus, removal of the C

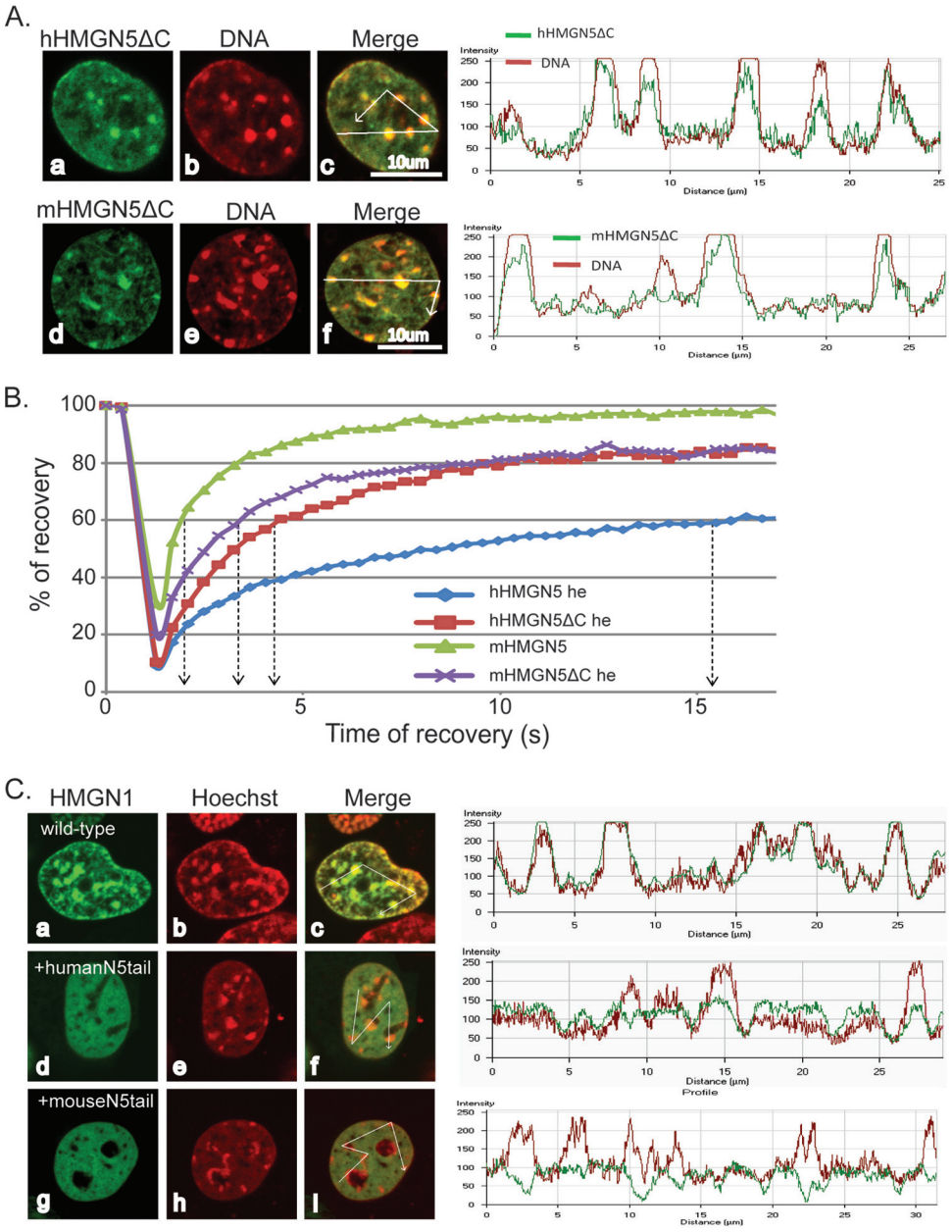

FIG. 4. The C terminus of HMGN5 determines the protein's chromatin localization. (A) Identical intranuclear locations of C-terminal deletion mutants of human and mouse HMGN5 proteins. Shown are mouse embryonic fibroblasts transfected with a YFP-labeled C-terminal deletion mutant of either human (a to c) or mouse (d to f) HMGN5. DNA was visualized by Hoechst staining. The merged images and their localization profiles indicate that the C-terminal deletion mutants of HMGN5 colocalized with heterochromatin (compact dots of DNA). (B) FRAP recovery curves for wild-type and C-terminal deletion (ΔC) mutant human and mouse HMGN5 proteins in either euchromatin or heterochromatin (he). Arrows point to the time needed for recovery of 60% of initial fluorescence (t_{60}). (C) Confocal images of MEFs expressing either HMGN1-YFP (a to c) or HMGN1 fused with the tail of human (d to f) or mouse (g to i) HMGN5.

terminus reduced the differences in chromatin interactions between the human and mouse HMGN5 proteins. Interestingly, while the human C-terminal domain strengthens the interaction of the respective native proteins with chromatin, the mouse C-terminal domain weakens it.

As a further test of the role of the C-terminal regions, we examined whether they can function as independent domains. To this end, we constructed expression vectors of HMGN1 fused to the tail of either mouse (amino acids 108 to 406) or human (amino acids 108 to 282) HMGN5. Both tails were labeled with green fluorescent protein (GFP). Confocal microscopy of mouse cells expressing either native HMGN1-GFP or the two constructs revealed differences in the locations of the proteins. As expected, native HMGN1 colocalized with the constitutive heterochromatin, which in Hoechst-stained cells appeared as discrete dots (Fig. 4C, panels a to c). Fusing the hHMGN5 tail to HMGN1 maintained the preference of the protein for heterochromatin (Fig. 4C, panels d to f and scan

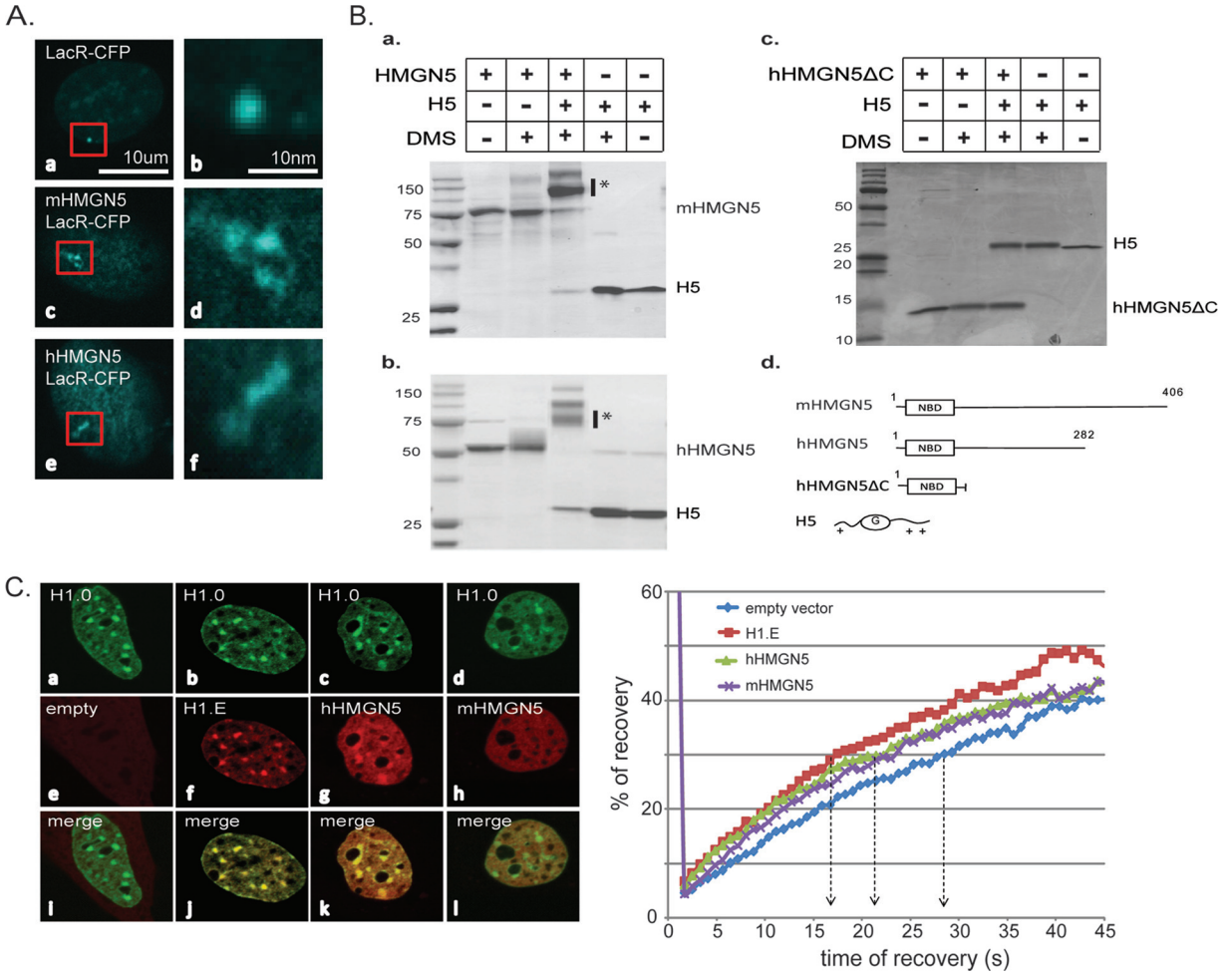

FIG. 5. HMGN5 interacts with linker histone H5 and decompacts chromatin. (A) HMGN5 induces large-scale chromatin decondensation. Shown are confocal images of cells harboring an array of 256 repeats of the Lac operator sequence which can bind multiple copies of Lac repressor (LacR) fused to either cyan fluorescent protein (CFP) (a and b), mouse HMGN5-CFP (c and d), or human HMGN5-CFP (e and f). The condensed array appears as a compact dot (a and b). The decondensed array appears as a larger structure (c to f). The right panels depict ×10 magnifications of the array. (B) *In vitro* cross-linking experiments with histone H5 and mouse HMGN5 (a), human HMGN5 (b), and a C-terminal deletion mutant of human HMGN5 (hHMGN5ΔC) (c). Proteins were cross-linked with DMS, and the complexes were analyzed by 15% SDS-PAGE. The reagents present in each mixture analyzed are indicated at the top. (d) Schematic representation of the proteins analyzed. G, globular domain of H5; *, cross-linked products. (C) HMGN5 reduces the chromatin binding of H1 *in vivo*. Mouse embryonic fibroblasts stably expressing H1.0-GFP were transfected with either empty vector or vectors expressing cherry-fused H1.E, hHMGN5, or mHMGN5. Confocal images of the transfected cells are shown in panels a to i. FRAP recovery curves for photobleached H1.0-GFP are shown on the right. Dotted lines point to the time needed for recovery of 30% of the initial H1.0-GFP fluorescence (t_{30}).

profiles). In contrast, when the mHMGN5 tail was fused to HMGN1, the fusion protein did not colocalize with heterochromatin (Fig. 4C, panels g to i and scan profiles).

In summary, the C-terminal domain of HMGN5 defines species-specific characteristics of the HMGN5 protein, such as the pattern of nuclear localization and the affinity of chromatin interaction.

Human HMGN5 interacts with linker histone H5 and decompacts chromatin. The differences in the properties of human and mouse HMGN5 proteins raise the possibility that the proteins are functionally distinct. We therefore tested whether hHMGN5 can induce chromatin reorganizations similar to those previously shown for mHMGN5 (32) by using the Lac repressor (LacR) system. Either human or mouse HMGN5 was expressed in NIH2/4 cells harboring an array of 256 repeats of the LacO sequence that can bind multiple copies of the Lac repressor (36). In this system, fusion of a protein of interest to LacR will tether it to the LacO sequence, thereby inducing alterations in the chromatin architecture of the array which can be detected by fluorescence microscopy. Expression of LacR-CFP revealed that the LacO array formed a small compact dot in the nucleus (Fig. 5A, panels a and b). In contrast, expression of either human or mouse HMGN5 fused with LacR-CFP led to significant chromatin decompaction, as demonstrated by the formation of larger and more extended structures (Fig. 5A, panels c to f). Thus, both human and mouse HMGN5 proteins induce global chromatin unfolding.

HMGN5-mediated chromatin decompaction may be due to the ability of HMGN5 to counteract the chromatin-condensing activity of the linker histone H1, as was shown for mouse

HMGN5 (32). To test whether hHMGN5 also interacts with H1, we used DMS to cross-link either purified mHMGN5, purified hHMGN5, or the deletion mutant hHMGN5ΔC, lacking the negatively charged C-terminal domain, with wild-type histone H5 (Fig. 5B, panel d). Analysis of the cross-linked products by electrophoresis on SDS-containing polyacrylamide gels indicated that both mHMGN5 (Fig. 5B, panel a) and hHMGN5 (Fig. 5B, panel b) interact with H5. Thus, whereas cross-linking of either hHMGN5, mHMGN5, or H5 by itself did not produce any cross-linked products, a mixture of H5 with either mHMGN5 or hHMGN5 formed high-molecular-weight bands indicative of cross-linked products (Fig. 5B, panels a and b). Significantly, a mixture of H5 and the hHMGN5ΔC deletion mutant did not result in specific cross-linked bands (Fig. 5B, panel c). We therefore concluded that the negatively charged C terminus of hHMGN5 interacts with the linker histone H5 in a fashion similar to that previously shown for mHMGN5 and HMGB1 (14).

Members of the HMGN protein family were shown to compete with histone H1 for chromatin binding sites in living cells (10). Since both human and mouse HMGN5 proteins interact with the linker histone H5 *in vitro*, we next tested whether they also affect the binding of the linker histone H1 to chromatin in living cells. To this end, we used FRAP in cells stably expressing the linker histone H1.0-GFP (25) to measure the mobility of H1.0-GFP following transient expression of mHMGN5, hHMGN5, and H1.E. The exogenous proteins were fused to mcherry (red fluorescence) to allow identification of the transfected cells. The fluorescence images indicate that while the exogenous H1.E and hHMGN5 proteins colocalized with H1.0-GFP, mHMGN5 did not, just as expected from previous analyses. To compare the relative mobilities of H1 in the presence of various competitors, we measured the time needed for recovery of 30% of the H1-GFP prebleach intensity (t_{30}). The FRAP recovery of H1 in cells transfected with control vector was relatively slow, with a t_{30} value of 28 s. Expression of exogenous H1.E reduced the t_{30} to 17 s, an indication that the H1.E variant efficiently competed with the H1-GFP variant and reduced its chromatin residence time. Expression of either mHMGN5 or hHMGN5 reduced the t_{30} to 22 s (Fig. 5C), confirming the ability of the HMGN5 proteins to compete with H1 for binding to chromatin. However, the competition between H1 and HMGN5 proteins was not as strong as the competition with H1 itself (22 s versus 28 s).

Distinct domains in HMGN5 inhibit the interaction of H1 with chromatin. The three structural domains contained in H1 (8) play distinct roles in the dynamic, multistep binding of H1 to chromatin (12, 38). The initial binding, which is metastable, occurs through the interaction of the highly positively charged H1 C-terminal domain with the negatively charged linker DNA, while in subsequent steps the globular domain of H1 binds near the nucleosomal dyad axis, leading to conformational changes and stabilization of compact chromatin structures (38). Given that the ability of HMGNs to reduce H1 binding to chromatin requires an intact HMGN nucleosome binding domain and that the C-terminal end of HMGN5 interacts with the positively charged C-terminal end of H1, it is possible that each HMGN5 domain could independently affect specific steps in the binding of H1 to chromatin.

We used FRAP analysis to test whether expression of HMGN5 or various HMGN5 mutants affects the chromatin interaction of H1 in living cells. Previous studies indicated that this approach is suitable for detecting competition between chromatin binding proteins for nucleosome binding sites (10). FRAP analysis indicated that both wild-type mHMGN5 and its C-terminally truncated form (mHMGN5ΔC), but not the mutated truncated form mHMGN5ΔC(S19,23E), inhibited the interaction of H1 with chromatin (Fig. 6A). Thus, as expected from previous analysis of HMGN1 and HMGN2, an HMGN protein with an intact c-NBD inhibits the binding of H1 to chromatin. Surprisingly, the mHMGN5(S19,23E) variant, with a mutated c-NBD, also inhibited the interaction of H1 with chromatin (Fig. 6A). Most likely, this inhibition was due to the interaction between the long C-terminal end of HMGN5 and the positively charged C-terminal end of H1. Indeed, the mHMGN5ΔC(S19,23E) mutant was ineffective at competing with H1 (compare lines 1 and 6 in Fig. 6A). Thus, the ability of HMGN5 to inhibit the interaction of H1 with chromatin is mediated by either the NBD or the C-terminal domain.

Since the negatively charged domain of HMGN5 interacts with the positively charged C terminus of H1 (Fig. 5), we postulated that this domain inhibits the initial, metastable binding of H1 to the linker DNA (see the model in Fig. 6C). The NBD of HMGNs interferes mainly with the second step of H1 binding to chromatin, which involves the globular domain of H1 (12, 38). Indeed, HMGN1 and HMGN2, which lack the long C terminus characteristic of HMGN5, interact with the dyad axis of the nucleosomal core particle (1). In summary, we concluded that HMGN5 competes with linker histone H1 by two different modes. In the first mode, HMGN5 affects the initial binding of H1 to chromatin via direct interaction with the C terminus, while in the second mode, the NBD competes with the second step of H1 binding to chromatin, i.e., with the binding of the globular domain of H1 near the dyad axis of the particle (Fig. 6C).

We next tested which of the domains are necessary to unfold chromatin, as measured by decompaction of the LacO array. We found that both wild-type mHMGN5 and the mHMGN5ΔC deletion mutant decompacted the array (Fig. 6B, panels b and d). In contrast, neither the double point mutant of the intact protein [mHMGN5(S19,23E)] nor the double point mutant of tailless HMGN5 [mHMGN5ΔC(S19,23E)] could unfold chromatin (Fig. 6B, panels c and e). Mutation of the two serines in the c-NBD has been shown to abolish the interaction of HMGNs with core particles (39). It follows that decompaction of the LacO array is contingent on the ability of HMGN to bind to the core particle.

Effects of human and mouse HMGN5 proteins on the cellular transcription profile. Since both the human and mouse HMGN5 proteins affect the binding of H1 to chromatin and alter the higher-order chromatin structure but localize to distinct chromatin domains, we tested whether they have similar or distinct effects on the cellular transcription profile. The effect of HMGN5 on transcription was tested in MDAMB231 cells, a human breast cancer cell line. These cells were selected because Western blot analyses indicated that they contain low levels of hHMGN5. We reasoned that the putative effects of exogenously expressed HMGN5 may be more obvious against a low background of endogenous protein. MDAMB231 clones stably overexpressing HMGN5 were obtained using a retrovi-

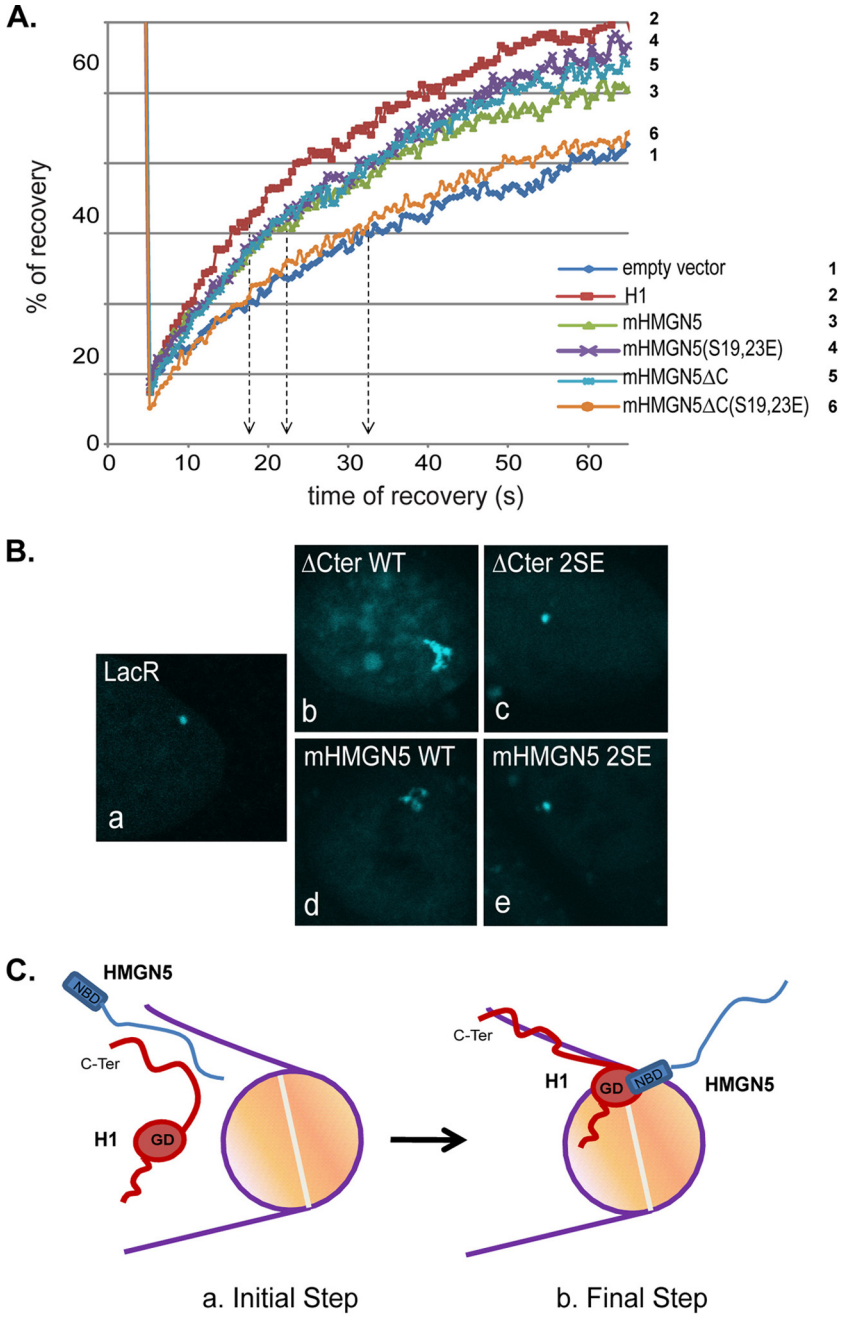

FIG. 6. Distinct domains in HMGN5 inhibit the interaction of H1 with chromatin. (A) Competitive FRAP analysis. Cells stably expressing H1.0-GFP were transfected with vectors expressing the indicated proteins, and the FRAP of H1.0-GFP was measured. (B) HMGN5-mediated chromatin decompaction. (a) Compact LacO array. Global chromatin decompaction by mHMGN5 (d) and mHMGN5ΔC (b), but not by the double point mutants HMGN5ΔC(S19,23E) (c) and mHMGN52S(S19,23E) (e), which do not bind to nucleosomes, is shown. (C) Model of HMGN5-mediated inhibition of H1-nucleosome interactions. In living cells, H1 binds dynamically to chromatin in a multistep process. (a) The first step is a metastable, low-affinity interaction of the positively charged C terminus of H1 with the negatively charged linker DNA. (b) In subsequent steps, the globular domain of H1 interacts with the nucleosome near the entry-exit point of the DNA. We postulate that HMGN5 can interfere with both steps. Step a is inhibited by the negatively charged C-terminal domain of HMGN5. Inhibition of step b requires efficient binding of the HMGN5 nucleosome binding domain to nucleosome core particles through the c-NBD.

rus-based expression system. Cells transfected with an empty retrovirus vector served as controls. Western analyses revealed that the transfected MDAMB231 cells expressed the exogenous proteins (Fig. 7A). The cellular transcription profiles were analyzed using Affymetrix expression arrays (see Materials and Methods). The resulting hierarchical dendrogram of the 3 array samples demonstrates that the profiles of gene expression are distinct (Fig. 7B).

Analysis of the changes in the transcription profiles ($P < 0.001$) indicated that expression of mHMGN5 and hHMGN5

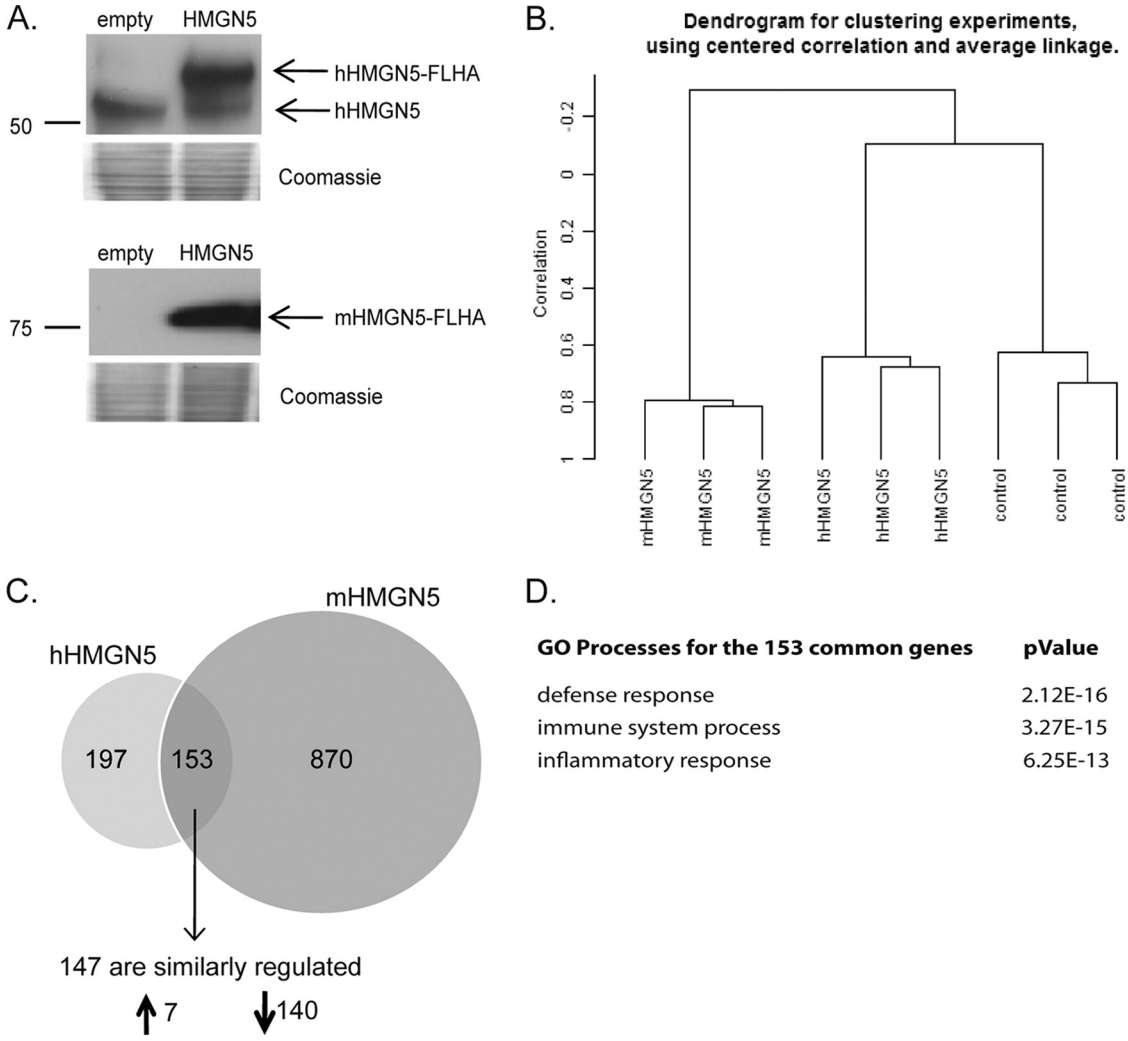

FIG. 7. HMGN5 effects on transcription. (A) Western blot analysis of MDAMB231 cells stably overexpressing hHMGN5 and mHMGN5. Coomassie blue staining indicates equal loading. (B) Clustering of the 3 arrays. (C) Venn diagram depicting the overlap of genes whose expression was altered by overexpressing either wild-type hHMGN5 or wild-type mHMGN5. The numbers of genes regulated similarly by both proteins are indicated. (D) Most significant gene ontology (GO) processes for the 153 common genes.

altered the levels of 1,023 genes and 350 genes, respectively, by approximately 2-fold (Fig. 7C). Among the 350 genes that were affected by hHMGN5, 153 were also affected by mHMGN5. Of these, 147 were similarly regulated: 7 genes were upregulated and 140 were downregulated by both the human and mouse HMGN5 proteins. Given the relatively low levels of hHMGN5 in MDAMB231 cells, the increase in the cellular level of the protein would not lead to major changes in the fraction of nucleosomes affected by the proteins. The number of genes affected by increased levels of mHMGN5 could be expected to be larger than that for genes affected by hHMGN5, since it localizes to euchromatin, which is significantly richer in transcriptionally active genes than heterochromatin, the target of hHMGN5. The relatively low levels of genes affected by the changes in HMGN5 levels are compatible with the notion that the protein affects the structure of chromatin and does not acts as a specific regulator of gene expression. Since HMGN5 is a structural protein, HMGN5-mediated transcriptional effects would be expected to be cell type specific and dependent on the cell type-specific chromatin organization and cell type-specific gene regulators. Indeed, the number of genes affected by exogenous expression of mHMGN5 in mouse AtT20 cells (32) or mouse embryonic fibroblasts (33) was different from that for genes affected in MDAMB231 cells.

DISCUSSION

The identification and characterization of novel HMGN variants are biologically significant because these proteins bind temporarily to nucleosomes, compete among themselves for binding sites, and also affect the binding of all linker histone H1 variants to chromatin (10, 13). Thus, these proteins function within a dynamic network in which the binding of all HMGN and H1 variants is interdependent. The evolution of a new HMGN variant can disrupt this network, ultimately affecting transcription and the cellular phenotype. In this respect, we note that human *HMGN5* is located at Xq13.3, a

region associated with mental retardation (Online Mendelian Inheritance in Man [OMIM] database).

The present work highlights the major similarities and differences between the human and mouse HMGN5 proteins. Our analyses indicate that the differences between the proteins are due mainly to their distinct C-terminal domains, which are encoded mostly by exon VI. This exon varies among all HMGN5 genes; it most likely evolves rapidly due to the presence of retrotransposon sequences inserted in the exon.

The C-terminal domains of both the mouse and human HMGN5 proteins have a highly disordered structure and a highly negative charge. Yet the C terminus of mouse HMGN5 prevents binding to constitutive heterochromatin, while the human HMGN5 C terminus does not. As a result, mHMGN5 binds mostly to CPs in euchromatin, while hHMGN5 seems to bind to heterochromatin. We note, however, that the localization profile of hHMGN5 mimics that of the DNA. Since the local density of the CPs is highest in heterochromatin, hHMGN5 seems to be targeted preferentially to that region, but in fact, it binds to CPs throughout the nucleus, just like all other HMGN variants except for mHMGN5.

Analysis of C-terminal truncation mutants of the mouse and human HMGN5 proteins and of domain swap mutants in which the C terminus of either mouse or human HMGN5 was fused to HMGN1 provided further proof of the importance of the C termini of the proteins. The localization profiles of the truncation mutants mimic that of the DNA, while the profiles of the swap mutants mimic that of the parent HMGN5 protein. The C terminus also affects the interaction of HMGN5 with CPs, as detected by FRAP analysis. FRAP can be used to measure the mobility of nuclear proteins in living cells, which on a first approximation is related to their binding dynamics in chromatin (37). The FRAP curves indicate that the chromatin residence time of mHMGN5 is significantly shorter than that of hHMGN5. Furthermore, while the fluorescence of mHMGN5 recovers fully, that of hHMGN5 does not, suggesting that a fraction of the protein is immobile. This difference in mobility between hHMGN5 and mHMGN5 is not due to the ability of the mouse protein to bind exclusively to the less condensed euchromatin fiber, because in this chromatin fraction the mobility of mHMGN5 is also significantly higher than that of hHMGN5 (Fig. 3, panel c). The differences are due to the properties of the C terminus, since the 2 truncated mutants, hHMGN5ΔC and mHMGN5ΔC, have very similar FRAP curves.

In spite of these differences, both human and mouse HMGN5 proteins interact with H1, inhibit its binding to chromatin, and can induce large-scale reorganization and unfolding of chromatin fibers. Furthermore, both proteins can alter gene expression, albeit mostly in a variant-specific manner. Since the mouse protein binds exclusively to the gene-rich euchromatin, its effects on transcription are more pronounced than those of the human variant. Given the similarity in the NBD of the human and mouse variants, it is likely that the transcriptional specificity of the proteins is due to their different C-terminal domains, which have a highly disordered structure (33). Since disordered proteins interact weakly with numerous partners (17, 24, 26), it is possible that each HMGN5 variant interacts preferentially with a specific set of partners and affects the expression of a unique set of genes. Therefore, a major future challenge is the identification of HMGN5 interacting partners.

ACKNOWLEDGMENTS

We thank Valarie Barr for technical assistance with microscopy and the NIH Fellows Editorial Board for editorial assistance. We thank G. Gerlitz for the H1.E-cherry plasmid.

This project was supported by the Center for Cancer Research intramural program of the NCI, NIH, under contract number N01-CO-12400.

REFERENCES

1. **Alfonso, P. J., M. P. Crippa, J. J. Hayes, and M. Bustin.** 1994. The footprint of chromosomal proteins HMG-14 and HMG-17 on chromatin subunits. J. Mol. Biol. **236:**189–198.
2. **Belova, G. I., Y. V. Postnikov, T. Furusawa, Y. Birger, and M. Bustin.** 2008. Chromosomal protein HMGN1 enhances the heat shock-induced remodeling of Hsp70 chromatin. J. Biol. Chem. **283:**8080–8088.
3. **Bianchi, M. E., and A. Agresti.** 2005. HMG proteins: dynamic players in gene regulation and differentiation. Curr. Opin. Genet. Dev. **15:**496–506.
4. **Birger, Y., et al.** 2005. Increased tumorigenicity and sensitivity to ionizing radiation upon loss of chromosomal protein HMGN1. Cancer Res. **65:**6711–6718.
5. **Bustin, M.** 2001. Chromatin unfolding and activation by HMGN(*) chromosomal proteins. Trends Biochem. Sci. **26:**431–437.
6. **Bustin, M.** 1999. Regulation of DNA-dependent activities by the functional motifs of the high-mobility-group chromosomal proteins. Mol. Cell. Biol. **19:**5237–5246.
7. **Bustin, M., F. Catez, and J. H. Lim.** 2005. The dynamics of histone H1 function in chromatin. Mol. Cell **17:**617–620.
8. **Bustin, M., and R. D. Cole.** 1970. Regions of high and low cationic charge in a lysine-rich histone. J. Biol. Chem. **245:**1458–1466.
9. **Bustin, M., and R. Reeves.** 1996. High-mobility-group chromosomal proteins: architectural components that facilitate chromatin function. Prog. Nucleic Acid Res. Mol. Biol. **54:**35–100.
10. **Catez, F., D. T. Brown, T. Misteli, and M. Bustin.** 2002. Competition between histone H1 and HMGN proteins for chromatin binding sites. EMBO Rep. **3:**760–766.
11. **Catez, F., and R. Hock.** 2010. Binding and interplay of HMG proteins on chromatin: lessons from live cell imaging. Biochim. Biophys. Acta **1799:**15–27.
12. **Catez, F., T. Ueda, and M. Bustin.** 2006. Determinants of histone H1 mobility and chromatin binding in living cells. Nat. Struct. Mol. Biol. **13:**305–310.
13. **Catez, F., et al.** 2004. Network of dynamic interactions between histone H1 and high-mobility-group proteins in chromatin. Mol. Cell. Biol. **24:**4321–4328.
14. **Cato, L., K. Stott, M. Watson, and J. O. Thomas.** 2008. The interaction of HMGB1 and linker histones occurs through their acidic and basic tails. J. Mol. Biol. **384:**1262–1272.
15. **Crippa, M. P., P. J. Alfonso, and M. Bustin.** 1992. Nucleosome core binding region of chromosomal protein HMG-17 acts as an independent functional domain. J. Mol. Biol. **228:**442–449.
16. **Ding, H. F., S. Rimsky, S. C. Batson, M. Bustin, and U. Hansen.** 1994. Stimulation of RNA polymerase II elongation by chromosomal protein HMG-14. Science **265:**796–799.
17. **Dunker, A. K., I. Silman, V. N. Uversky, and J. L. Sussman.** 2008. Function and structure of inherently disordered proteins. Curr. Opin. Struct. Biol. **18:**756–764.
18. **Hofmann, K., P. Bucher, L. Falquet, and A. Bairoch.** 1999. The PROSITE database, its status in 1999. Nucleic Acids Res. **27:**215–219.
19. **Khil, P. P., B. Oliver, and R. D. Camerini-Otero.** 2005. X for intersection: retrotransposition both on and off the X chromosome is more frequent. Trends Genet. **21:**3–7.
20. **Kim, Y. C., et al.** 2009. Activation of ATM depends on chromatin interactions occurring before induction of DNA damage. Nat. Cell Biol. **11:**92–96.
21. **King, L. M., and C. A. Francomano.** 2001. Characterization of a human gene encoding nucleosomal binding protein NSBP1. Genomics **71:**163–173.
22. **Lim, J. H., et al.** 2004. Chromosomal protein HMGN1 modulates histone H3 phosphorylation. Mol. Cell **15:**573–584.
23. **Lim, J. H., et al.** 2005. Chromosomal protein HMGN1 enhances the acetylation of lysine 14 in histone H3. EMBO J. **24:**3038–3048.
24. **Lu, X., B. Hamkalo, M. H. Parseghian, and J. C. Hansen.** 2009. Chromatin condensing functions of the linker histone C-terminal domain are mediated by specific amino acid composition and intrinsic protein disorder. Biochemistry **48:**164–172.
25. **Misteli, T., A. Gunjan, R. Hock, M. Bustin, and D. T. Brown.** 2000. Dynamic binding of histone H1 to chromatin in living cells. Nature **408:**877–881.
26. **Oldfield, C. J., et al.** 2008. Flexible nets: disorder and induced fit in the associations of p53 and 14-3-3 with their partners. BMC Genomics **9**(Suppl. 1)**:**S1.
27. **Postnikov, Y., and M. Bustin.** 2010. Regulation of chromatin structure and function by HMGN proteins. Biochim. Biophys. Acta **1799:**62–68.

28. **Postnikov, Y. V., and M. Bustin.** 1999. Reconstitution of high mobility group 14/17 proteins into nucleosomes and chromatin. Methods Enzymol. **304:**133–155.
29. **Postnikov, Y. V., L. Trieschmann, A. Rickers, and M. Bustin.** 1995. Homodimers of chromosomal proteins HMG-14 and HMG-17 in nucleosome cores. J. Mol. Biol. **252:**423–432.
30. **Rattner, B. P., T. Yusufzai, and J. T. Kadonaga.** 2009. HMGN proteins act in opposition to ATP-dependent chromatin remodeling factors to restrict nucleosome mobility. Mol. Cell **34:**620–626.
31. **Rochman, M., C. Malicet, and M. Bustin.** 2010. HMGN5/NSBP1: a new member of the HMGN protein family that affects chromatin structure and function. Biochim. Biophys. Acta **1799:**86–92.
32. **Rochman, M., et al.** 2009. The interaction of NSBP1/HMGN5 with nucleosomes in euchromatin counteracts linker histone-mediated chromatin compaction and modulates transcription. Mol. Cell **35:**642–656.
33. **Rochman, M., et al.** Effects of HMGN variants on the cellular transcription profile. Nucleic Acids Res., in press.
34. **Shirakawa, H., D. Landsman, Y. V. Postnikov, and M. Bustin.** 2000. NBP-45, a novel nucleosomal binding protein with a tissue-specific and developmentally regulated expression. J. Biol. Chem. **275:**6368–6374.
35. **Shirakawa, H., et al.** 2009. The nucleosomal binding protein NSBP1 is highly expressed in the placenta and modulates the expression of differentiation markers in placental Rcho-1 cells. J. Cell Biochem. **106:**651–658.
36. **Soutoglou, E., and T. Misteli.** 2008. Activation of the cellular DNA damage response in the absence of DNA lesions. Science **320:**1507–1510.
37. **Sprague, B. L., and J. G. McNally.** 2005. FRAP analysis of binding: proper and fitting. Trends Cell Biol. **15:**84–91.
38. **Stasevich, T. J., F. Mueller, D. T. Brown, and J. G. McNally.** 2010. Dissecting the binding mechanism of the linker histone in live cells: an integrated FRAP analysis. EMBO J. **29:**1225–1234.
39. **Ueda, T., F. Catez, G. Gerlitz, and M. Bustin.** 2008. Delineation of the protein module that anchors HMGN proteins to nucleosomes in the chromatin of living cells. Mol. Cell. Biol. **28:**2872–2883.
40. **Vandepoele, K., W. De Vos, J. S. Taylor, A. Meyer, and Y. Van de Peer.** 2004. Major events in the genome evolution of vertebrates: paranome age and size differ considerably between ray-finned fishes and land vertebrates. Proc. Natl. Acad. Sci. U. S. A. **101:**1638–1643.
41. **Vestner, B., M. Bustin, and C. Gruss.** 1998. Stimulation of replication efficiency of a chromatin template by chromosomal protein HMG-17. J. Biol. Chem. **273:**9409–9414.
42. **Woodcock, C. L., A. I. Skoultchi, and Y. Fan.** 2006. Role of linker histone in chromatin structure and function: H1 stoichiometry and nucleosome repeat length. Chromosome Res. **14:**17–25.
43. **Zhu, N., and U. Hansen.** 2010. Transcriptional regulation by HMGN proteins. Biochim. Biophys. Acta **1799:**74–79.